International Journal of Mechanical Sciences 85 (2014) 104–109

Contents lists available at ScienceDirect

International Journal of Mechanical Sciences

journal homepage: www.elsevier.com/locate/ijmecsci

Effect of contact angle on contact morphology and Vickers hardness measurement in instrumented indentation testing

Seung-Kyun Kang [a], Young-Cheon Kim [b], Jin-Woo Lee [c], Dongil Kwon [c], Ju-Young Kim [b,d,*]

[a] Department of Materials Science and Engineering, Frederick Seitz Materials Research Laboratory, University of Illinois at Urbana-Champaign, Urbana, IL 61801, USA
[b] School of Materials Science and Engineering, UNIST (Ulsan National Institute of Science and Technology), Ulsan 689-798, Republic of Korea
[c] Department of Materials Science and Engineering, Seoul National University, Seoul 151-744, Republic of Korea
[d] KIST-UNIST Ulsan Center for Convergent Materials, UNIST (Ulsan National Institute of Science and Technology), Ulsan 689-798, Republic of Korea

A R T I C L E I N F O

Article history:
Received 25 December 2013
Received in revised form
28 April 2014
Accepted 2 May 2014
Available online 20 May 2014

Keywords:
Contact angle
Contact morphology
Vickers hardness
Scaling relation
Instrumented indentation

A B S T R A C T

We derive a general contact-depth function for the Vickers indenter by modifying a scaling relation between yield strain and indentation depth ratio, which is comprised of indenter angle, plastic constraint factor, and indentation depth ratio. The validity of this function is demonstrated by using various indenters of different angles. A method for calibrating the actual contact area of an imperfectly shaped Vickers indenter is suggested that yields a better evaluation of Vickers hardness in the instrumented indentation test.

1. Introduction

Understanding contact morphology is a fundamental issue in instrumented indentation testing. While Hertz's elastic contact solution has been generally used for various indenter geometries, plastic deformation underneath an indenter is not fully described by an analytical solution. Among suggested plasticity models in indentation, Johnson's expanding-cavity model is among the most commonly used [1]. Johnson extended Hill's spherical cavity model [1] to indentation contact problems by assuming a hemispherical cavity field underneath the indenter, which provided a good approximation to the stress–strain field under an indenter. However, it assumes conservation conditions, i.e. that the penetrated volume is the same as the expanding cavity volume; thus it does not allow for the effect of stress flow in inducing plastic pileup around the indenter. Describing material pileup around the indenter with simple analytic methods only is challenging, so much work has been performed using parametric analysis or/and computational simulation, generally finite element analysis (FEA) [2–13].

Cheng and Cheng suggested parametric analysis using FEA and proposed dominant instrumented indentation parameters determining material pileup to be (1) yield strain (ratio of yield strength to elastic modulus, σ_y/E), (2) indenter half-angle θ as described in Figs. 1, and (3) the strain-hardening exponent n. The average strain under the indenter is a constant regardless of indentation depth for a sharp geometrically self-similar indenter, and thus when the total strain is fixed for sharp indenter, the amount of plastic strain decreases as the yield strain increases. For a sharp indenter, the smaller θ induces higher total strain in materials so there may be plenty of room for greater plastic strain. The effect of the strain-hardening exponent n on materials pileup can be explained by the relative ease of propagating deformation to the undeformed zone; a higher strain-hardening exponent means that the strain-hardened deformed region becomes much harder than the neighboring undeformed region, resulting in less material pileup due to easier plastic flow [16–17].

We found that the yield strain is a primary factor determining material pileup among yield strain and strain-hardening exponent in Vickers indentations for 24 metallic materials [16]. We defined a contact-depth function f as

$$f = \frac{h_c}{h_{max}} = \frac{h_{max} - h_d + h_p}{h_{max}}, \tag{1}$$

where h_c is the contact depth that reflects elastic deflection h_d and plastic pileup h_p and h_{max} is the maximum indentation depth from the initial surface, as described in Fig. 1 (It is noteworthy that

* Corresponding author at: UNIST (Ulsan National Institute of Science and Technology), School of Materials Science and Engineering, Ulsan 689-798, Republic of Korea.
E-mail address: juyoung@unist.ac.kr (J.-Y. Kim).

http://dx.doi.org/10.1016/j.ijmecsci.2014.05.002
0020-7403/

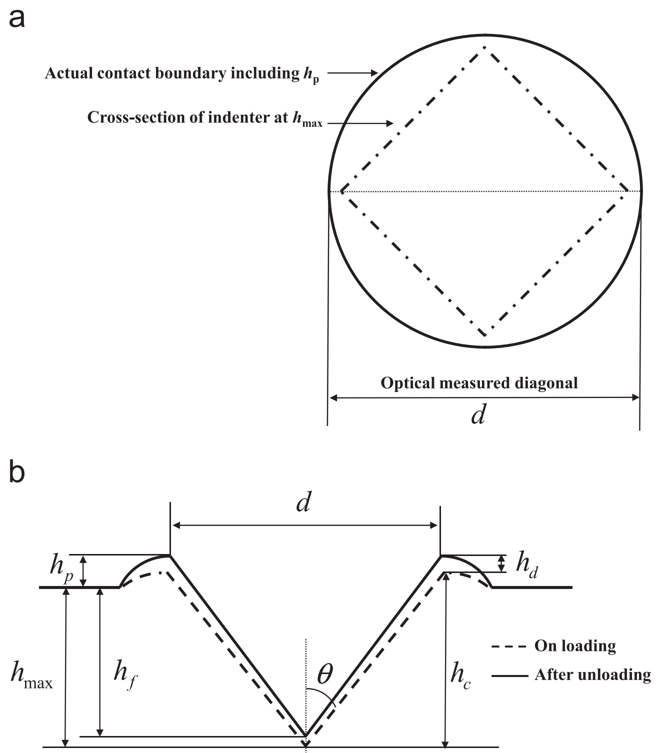

Fig. 1. Contact morphology of Vickers indentation: (a) top side view and (b) cross-sectional view.

although the actual pileup height is identical during unloading, this pileup height seems to increase due to elastic recovery of elastic deflection.) [18–21]. Experimental results show a linear relation between contact-depth function f and the inverse of the yield strain [16]:

$$f = a'\left(\frac{\sigma_y}{E_r}\right)^{-1} + b', \tag{2}$$

where a' and b' are constants, σ_y is the yield strength, and E_r is the reduced elastic modulus in instrumented indentation [19]. By the simple approximation that $H=\psi\sigma_y$, where H is the hardness and ψ is the plastic constraint factor, the yield strain can be replaced by the ratio of hardness to reduced elastic modulus H/E_r [16]. The scaling indentation relation between ratio of hardness to reduced elastic modulus H/E_r and elastic indentation energy ratio $W_{elastic}/W_{total}$, where $W_{elastic}$ is elastically stored work and W_{total} is total work induced during indentation, was used to evaluate the contact-depth function using indentation parameters only. Finally, the contact-depth function for projected area is determined from the maximum indentation depth and final indentation depth (h_f) as [16,17]

$$f = 1.06 \times 10^{-2}\frac{h_{max}}{h_{max}-h_f} + 1.00. \tag{3}$$

The contact-depth function for Vickers indenter f_V is determined by a similar derivation as

$$f_V = \frac{h_c^V}{h_{max}} = 9.90 \times 10^{-3}\frac{h_{max}}{h_{max}-h_f} + 1.00, \tag{4}$$

where h_c^V is the contact depth at the edge of the residual impression in Vickers indentation [16,17]. Eqs. (3) and (4) show that f and f_V are described by the ratio of indentation depths. Here the definitions of contact area and hence hardness differ in instrumented indentation and Vickers indentation. Hardness in instrumented indentation (H) uses the projected area as the nominal area; however, Vickers hardness (HV) uses the surface area of the Vickers indenter and calculates the area from the corner-to-corner length only. The conventional Vickers hardness is widely used for its simplicity, but in this paper, the derivation is on the basis of hardness in instrumented indentation so as to consider the pileup effects.

Here we suggest a theoretical analysis for the contact-depth function by investigating a scaling relation between yield strain and indentation depth ratio for the actual contact depth in Vickers indentation. We investigate the effects of material properties and sharp indenter angles on materials pileup. By combining theoretical analysis and experimental results, including the effects of material properties and sharp indenter angle on material pileup, we propose a novel way to determine contact-depth function and Vickers hardness.

2. Material and experimental details

Twenty-five metallic specimens (carbon steels – S20, S45C, SCM21, SCM4, SKD61, SKS3, SUJ2, API X70, API X100; stainless steels – SUS303F, SUS310S, SUS316L, SUS403, SUS410, SUS420J2; Ni alloy – Inconel 600; Al alloys – Al6061, Al7075; copper alloys – C1010, C5101, C62400; Ti alloys – Ti-10V–2Fe–3Al, Ti–7Al–4Mo) were prepared and polished gently with 1 μm diamond powder. Instrumented indentation testing was performed with an AIS System (FRONTICS, Korea) with force resolution 55 mN and displacement resolution 100 nm; three different four-sided pyramidal indenters with half-angles of 56.5°, 68.0°, and 75.8° were used. The indentation tests were performed with maximum indentation depth 80 μm at constant displacement rate 0.3 mm/min. The instruments were calibrated by the standard calibration procedure [22]. Residual indentation impressions were optically measured to evaluate contact depth from real contact area (A_c). The contact depth and contact area have the following geometrical relationship depending on the indenter half-angle for a pyramidal indenter:

$$h_c = \frac{\sqrt{A_c}}{2\ \tan\ \theta} \tag{5}$$

for a Vickers indenter, $\theta=68°$. The hardness in instrumented indentation, defined as P/A_c, is measured by the maximum load of instrumented indentation and the contact area as found by optical microscopy. The reduced elastic modulus was calculated as $\sqrt{\pi}S/2\sqrt{A_c}$, where S is the initial unloading slope measured from the unloading curve of instrumented indentation. The yield strength was measured by tension testing with cylindrical specimens of 25 mm length and 6 mm diameter.

We prepared standard hardness blocks of Vickers hardness 150, 200, 300 and 500 (Yamamoto Scientific Tool Laboratory Co., Ltd. Chiba, Japan) respectively, and three different commercial Vickers indenters (A.L.M.T. Co. Tokyo, Japan) to calibrate the contact-depth function depending on the geometrical imperfection of the indenters. Indentation was performed on standard hardness blocks for three different Vickers indenters and with maximum indentation depth of 80 μm. The diagonal lengths of residual indentation impressions d were measured by an optical microscope. Using the following relation in Vickers hardness (HV), we can derive h_c^V from d or HV by

$$HV = 1.8544P/d^2, \tag{6}$$

$$h_c^V = d/7, \tag{7}$$

where P is the maximum indentation load.